chosen numbers. We analyzed the $N \times N$ covariance map of electron signals collected from the N Rydberg states to discover which states were flipped. We retrieved the correct number 96% of the time for $N = 6$ and 80% for $N = 8$. These results are summarized in Fig. 3.

One need not confine information storage to $M = 2$ quantum phases per state. In previous work, we demonstrated quantum phase sensitivity for Rydberg wave packets of $\lesssim$10%, which means that more than 30 different numbers can be mapped in a single state (*13*). The maximum number stored in 20 states then reaches $30^{20} \approx 2^{100}$. Other algorithms can be implemented by other unitary transformations such as the application of ultrafast shaped terahertz pulses (*14*). Entanglement of additional degrees of freedom, such as spin and orbital angular momentum, will also extend the reach of this system.

References and Notes

1. D. Deutsch, *Proc. R. Soc. London Ser. A* **400**, 97 (1985).
2. B. Schumacher, *Phys. Rev. A* **51**, 2738 (1995).
3. C. H. Bennett, *Phys. Today* **48** (October), 24 (1995).
4. L. K. Grover, *Phys. Rev. Lett.* **79**, 325 (1997).
5. ———, *Phys. Rev. Lett.* **79**, 4709 (1997).
6. S. Lloyd, Los Alamos National Laboratory e-print quant-ph/9903057 (1999).
7. J. A. Jones, M. Mosca, R. H. Hansen, *Nature* **393**, 344 (1998).
8. I. L. Chuang, N. Gershenfeld, M. Kubinec, *Phys. Rev. Lett.* **80**, 3408 (1998).
9. P. G. Kwiat, J. R. Mitchell, P. D. D. Schwindt, A. G. White, Los Alamos National Laboratory e-print quant-ph/9905086 (1999).
10. D. Strickland and G. Mourou, *Opt. Commun.* **55**, 447 (1985).
11. J. X. Tull, M. A. Dugan, W. S. Warren, *Adv. Opt. Magn. Reson.* **20**, 1 (1997).
12. T. F. Gallagher, L. M. Humphrey, W. E. Cooke, R. M. Hill, S. A. Edelstein, *Phys. Rev. A* **16**, 1098 (1977).
13. T. C. Weinacht, J. Ahn, P. H. Bucksbaum, *Phys. Rev. Lett.* **80**, 5508 (1998).
14. N. E. Tielking and R. R. Jones, *Phys. Rev. A* **52**, 1371 (1995).

15. Supported by NSF grant 9414335.

5 October 1999; accepted 16 November 1999

Mirrorless Lasing from Mesostructured Waveguides Patterned by Soft Lithography

Peidong Yang,[1]*† Gernot Wirnsberger,[1]* Howard C. Huang[1,2] Steven R. Cordero,[1] Michael D. McGehee,[1,3] Brian Scott,[1] Tao Deng,[4] George M. Whitesides,[4] Bradley F. Chmelka,[2] Steven K. Buratto,[1] Galen D. Stucky[1,3]‡

Mesostructured silica waveguide arrays were fabricated with a combination of acidic sol-gel block copolymer templating chemistry and soft lithography. Waveguiding was enabled by the use of a low–refractive index (1.15) mesoporous silica thin film support. When the mesostructure was doped with the laser dye rhodamine 6G, amplified spontaneous emission was observed with a low pumping threshold of 10 kilowatts per square centimeter, attributed to the mesostructure's ability to prevent aggregation of the dye molecules even at relatively high loadings within the organized high–surface area mesochannels of the waveguides. These highly processible, self-assembling mesostructured host media and claddings may have potential for the fabrication of integrated optical circuits.

Acidic sol-gel self-assembly chemistry (*1–3*) is particularly useful in synthesizing inorganic-organic composite mesoscopically ordered films, fibers, monoliths, and hierarchically ordered structures (*4–9*). Applications of mesoporous materials, for example, as catalysts and separation membranes, have been the main driving force in this field, and their performance in these respects has been extensively documented (*10*). Rather unexplored is the possibility of using mesostructured materials for advanced optical applications. Because of their mesoscopically ordered structures, these materials represent ideal hosts for encapsulating dyes, polymers, and nanocrystals to produce complex multicomponent hybrid materials with interesting and useful optical properties (*11–13*).

We report the fabrication of mesostructured waveguides that exhibit amplified spontaneous emission (ASE), a type of mirrorless lasing (*14*), on low–refractive index mesoporous SiO_2 claddings. A one-step, self-assembly process was achieved by the combination of acidic sol-gel block copolymer templating chemistry with the soft lithographic techniques micromolding, micromolding in capillaries (MIMIC), and microtransfer molding, which have previously been shown to allow the rapid and inexpensive fabrication of liquid-core, polymeric, and inorganic waveguides (*15–17*). In each case, a poly(dimethylsiloxane) (PDMS) elastomeric mold was used to control the shape of the waveguide, whereas block copolymers were used to control the mesostructure.

For waveguiding to occur, the refractive index of the waveguiding medium must be higher than that of its surroundings. Because the mesostructured silica has a refractive index of only 1.43, silicon wafers (refractive index 3.5) coated with mesoporous silica were used as substrates; mesoporous silica is an excellent cladding material because it is mechanically and hydrothermally stable and has a refractive index of only 1.15 (Fig. 5A). The use of these block polymer–derived porous silica materials as low-index-of-refraction silica supports is a convenient route for interfacing the more traditional solid glass, liquid-core, and even polymer waveguides.

To make patterned mesostructures, using MIMIC as an example, we cut open the PDMS stamp at both ends and placed it on a substrate to establish conformal contact. A drop of sol-gel–block copolymer solution (*9, 18*) was then placed at one end of the open microchannels, which were subsequently filled by capillary flow. Gelation of the mesophase precursor solution normally occurred within a few hours. The mold and the resulting mesostructure were left undisturbed for at least 12 hours to allow increased cross-linking and consolidation of the silica network. Then the stamp was peeled off, and the substrate was cleaved to remove the thick film regions on areas that had not been covered by the stamp.

Scanning electron microscope (SEM) images of these patterned mesostructures show line arrays (Fig. 1A) several centimeters long, 1 to 3 μm wide, and 1 to 2 μm high, with 2- to 8-μm spacing. More complex structures with possible optical applications may be fabricated by the use of Fresnel lenses and diffraction gratings as masters to make PDMS molds. These PDMS molds can then be used, for example, to fabricate mesostructured curve or ring patterns (Fig. 1B). The high diversity and complexity of the structures that can be fabricated with the current process offer attractive possibilities for making various optical devices with different functionalities (*9*).

Mesoscopic ordering in the patterned silica-copolymer materials was characterized by low-angle x-ray diffraction (XRD). The

[1]Department of Chemistry, [2]Department of Chemical Engineering, [3]Department of Materials, University of California, Santa Barbara, CA 93106, USA. [4]Department of Chemistry, Harvard University, Cambridge, MA 02138, USA.

*These authors contributed equally to this work.
†Present address: Department of Chemistry, University of California, Berkeley, CA 94720, USA.
‡To whom correspondence should be addressed. E-mail: stucky@chem.ucsb.edu

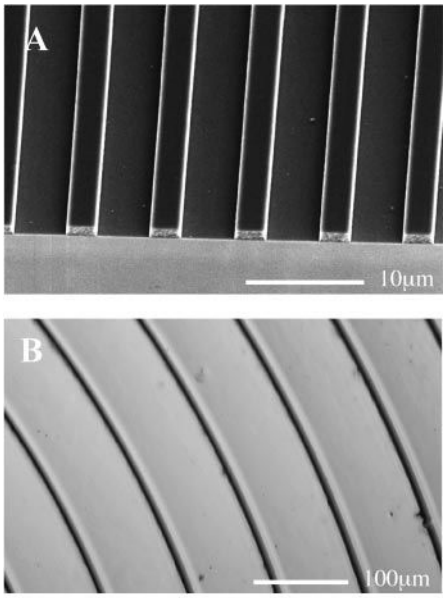

Fig. 1. SEM images of hexagonal mesostructured silica-$EO_{20}PO_{70}EO_{20}$ composite arrays. (**A**) Line arrays fabricated with MIMIC and (**B**) circular patterns fabricated with microtransfer molding.

block copolymer P123 used in this study favors the formation of a hexagonal mesophase. In the low-angle XRD patterns (Fig. 2), only (001) peaks are observed, indicating that the mesoscaled channels are parallel to the substrate. In addition, the variations of the diffraction peak intensity when rotating the sample azimuthally indicate that the mesostructured channels are partially aligned along the axes of the microchannels (*19*), consistent with the proposition that the formation of end caps in self-assembled surfactant cylinders is not energetically favored given their high free energy of formation (*20*).

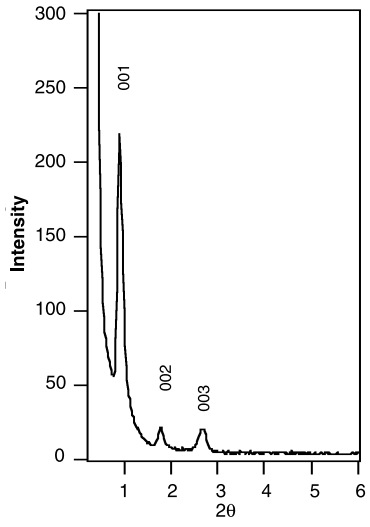

Fig. 2. Low-angle XRD pattern of the hexagonal mesostructured arrays showing only (001) peaks, indicating that the mesoscale channels are aligned parallel to the substrate plane (*6*).

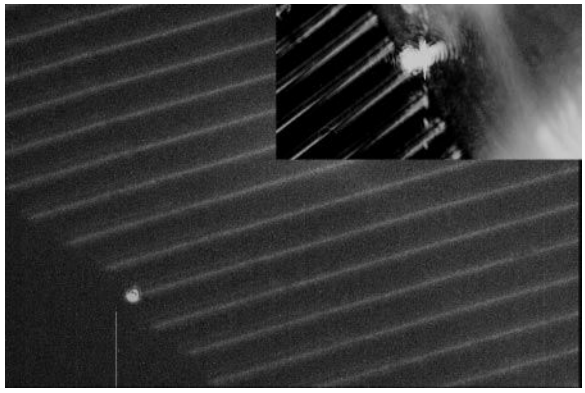

Fig. 3. Optical images demonstrating the waveguiding capability of the patterned mesostructured silica composite arrays. The inset shows the single-mode optical fiber used to couple light into an individual waveguide. Each waveguide has a width of 2.4 μm.

To demonstrate waveguiding, an important basic property for optical applications, we mounted a line-patterned sample (Fig. 1A) on a micromanipulator stage and used a single-mode optical fiber to couple He-Ne laser light into one of the cleaved waveguides. The sample was translated with a micromanipulator, and the guided output was imaged with a charge-coupled device (CCD) camera mounted on an optical microscope. Typical images of a 0.5-mm-long waveguide array (Fig. 3) show no scattering along the waveguides and strong emission from the ends, indicating that the waveguides are of high quality. Efficient waveguiding was also observed in curved stripes. The capability of guiding optical signals with these patterned mesostructures is essential for their incorporation into integrated optical circuits.

To explore the possibility of using mesostructures as host media for the one-step assembly of advanced optical components, such as lasers, we doped waveguide arrays with the laser dye rhodamine 6G (Rh6G) during their synthesis. Imaging of photoluminescence (PL) by laser scanning confocal microscopy was used to probe the distribution of the dye molecules. The uniform intensity of the PL (Fig. 4) indicates that the dye molecules are uniformly distributed within the mesostructured host medium.

To demonstrate the ability of the waveguides to amplify light, we optically pumped a line-patterned array by a frequency-doubled neodymiun–yttrium-aluminum-garnet laser (532 nm, 10 Hz, about 10 ns pulse width). A beam stripe of 1.5 mm was selected by an adjustable slit and focused with a cylindrical lens to a width of about 0.5 mm. The incident light was perpendicular to the substrate surface, and the axial emission, emitted from the end of the waveguides, was detected with a monochromator (150 grooves/mm) and a thermoelectrically cooled CCD detector (Fig. 5A). At low pump intensities (0.8 kW cm^{-2}), a broad PL spectrum was observed (Fig. 5A) with a full width at half maximum of around 50 nm and a peak maximum at 586 nm. When the pump intensity was increased above 10 kW cm^{-2}, the PL intensity at 577 nm grew superlinearly, and the spectral width decreased to 7 nm. This behavior is indicative of ASE, a process in which spontaneously emitted photons are amplified by stimulated emission as they travel through a gain medium (*14*, *21*). Further evidence for ASE was obtained by varying the length of the pump stripe. It was found that the output intensity increased exponentially and the spectral width decreased as the length was increased. Figure 5C shows the intense edge emission from the waveguides that results when ASE occurs. The observation of ASE at low thresholds demonstrates that lasers with coherent emission could be made if mirrors were incorporated to provide feedback.

There are several reports on nonepitaxially grown materials, such as polymers (*22*) or liquid microdroplets (*23*), that exhibit ASE or laser emission. From the perspective of device

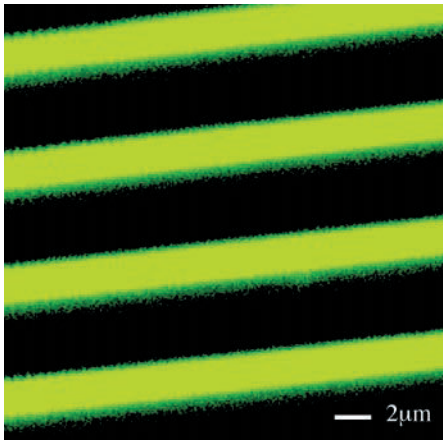

Fig. 4. Laser scanning confocal microscopy images of Rh6G-doped silica-$EO_{20}PO_{70}EO_{20}$ mesostructured arrays. The excitation source, the 514-nm line of an Ar^{+} laser, was directed into a high–numerical aperture (NA) air objective (NA = 0.8) and focused to a small spot (~500 nm) on the sample. The fluorescence was collected with the same objective and passed through a holographic notch filter to remove scattered laser light. An image is formed point by point by raster scanning the sample with commercial scanning electronics. The image indicates that the dye molecules are uniformly distributed within the resolution of our microscope.

feasibility and applications, however, solid state materials with mechanical and thermal robustness and high photostability are desired. Subnanostructured materials such as zeolites fulfill these criteria, but they have only limited macroscopic processibility (*24*). Another attractive choice from the consideration of rapid processing and thermal and mechanical stability is sol-gel glasses, which have previously been used as host media for solid state Rh6G dye lasers (*25*, *26*). To compare our materials with dye-doped sol-gel glasses, we prepared Rh6G-doped SiO_2 sol-gel glasses with the same compositional range, but without the mesostructure-directing surfactants. Although we could also observe ASE for these materials, their thresholds were an order of magnitude higher (around 200 kW cm^{-2}), in agreement with the relatively high thresholds reported for amorphous sol-gel–derived TiO_2-SiO_2 films (*27*).

The limitation on the ASE threshold in the sol-gel glasses is that low dye concentrations must be used to prevent dimerization, which lowers quantum efficiency (*28*). Lower thresholds can be achieved with the mesostructured waveguides because the block copolymers control the dye arrangement in such a way that dimerization is suppressed (*29*). The ultraviolet-visual absorption spectra of films with 0.5 weight % Rh6G in mesostructured silica and in sol-gel glasses were measured. It was found that the spectra from the mesostructured films resemble that of dilute Rh6G in ethanol but that the spectrum of the sol-gel glasses shows features that are characteristic of dimer absorption. Hence, the mesostructured waveguides are not only easy to fabricate, but they also enhance the emissive properties of the dyes that they contain by preventing concentration quenching. Work is in progress to determine how the dye molecules are arranged within the mesostructures.

In summary, coassembled mesostructures are a promising class of optical materials. Mesoporous films are useful as claddings because of their low refractive indices. Mesostructured silica-polymer films are a good host for laser dyes, such as Rh6G, because a large concentration of a dye can be incorporated without concentration quenching. We observed mirrorless lasing (ASE) at a pump intensity of only 10 kW cm^{-2}. We anticipate that many other dye molecules (*30*), rare-earth complexes, or nanocrystals can be incorporated into mesostructures to obtain different optical properties and functionalities by the rational tuning of the host architecture, the orientation and alignment of the guest species, and the host-guest interactions. The combination of acidic sol-gel block copolymer templating chemistry and soft lithography enables the patterning of waveguides and other optical components in a highly processible, inexpensive, and reproducible fashion.

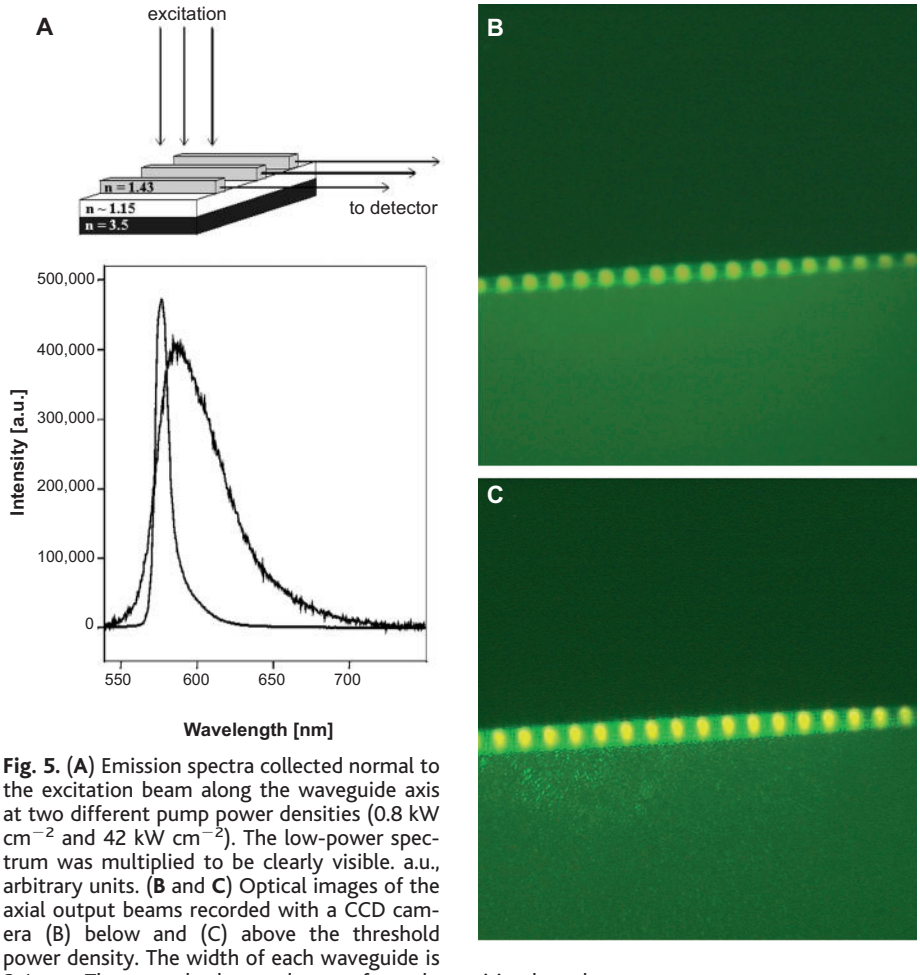

Fig. 5. (**A**) Emission spectra collected normal to the excitation beam along the waveguide axis at two different pump power densities (0.8 kW cm^{-2} and 42 kW cm^{-2}). The low-power spectrum was multiplied to be clearly visible. a.u., arbitrary units. (**B** and **C**) Optical images of the axial output beams recorded with a CCD camera (B) below and (C) above the threshold power density. The width of each waveguide is 2.4 μm. The green background stems from the exciting laser beam.

References and Notes

1. Q. Huo *et al.*, *Nature* **368**, 317 (1994).
2. Q. Huo *et al.*, *Chem. Mater.* **6**, 1176 (1994).
3. D. Zhao *et al.*, *Science* **279**, 548 (1998).
4. H. Yang, N. Coombs, G. A. Ozin, *Nature* **385**, 692 (1997).
5. Y. Lu *et al.*, *Nature* **389**, 364 (1997).
6. D. Zhao, P. Yang, J. Feng, B. F. Chmelka, G. D. Stucky, *Adv. Mater.* **10**, 1380 (1998).
7. P. Yang, D. Zhao, B. F. Chmelka, G. D. Stucky, *Chem. Mater.* **10**, 2033 (1998).
8. N. Melosh *et al.*, *Macromolecules* **32**, 4332 (1999).
9. P. Yang *et al.*, *Science* **282**, 2244 (1998).
10. A. Corma, *Chem. Rev.* **97**, 2373 (1997).
11. V. I. Srdanov, I. Alxneit, G. D. Stucky, C. M. Reaves, S. P. DenBaars, *J. Phys. Chem. B* **102**, 3341 (1998).
12. F. Marlow, M. D. McGehee, D. Zhao, B. F. Chmelka, G. D. Stucky, *Adv. Mater.* **11**, 632 (1999).
13. C.-G. Wu and T. Bein, *Science* **264**, 1757 (1994).
14. A. E. Siegmann, *Lasers* (University Science Books, Mill Valley, CA, 1986).
15. X. Zhao, S. P. Smith, S. J. Waldman, G. M. Whitesides, M. Prentiss, *Appl. Phys. Lett.* **71**, 1017 (1997).
16. O. J. A. Schueller, X. Zhao, G. M. Whitesides, S. P. Smith, M. Prentiss, *Adv. Mater.* **11**, 37 (1999).
17. C. Marzolin, S. P. Smith, M. Prentiss, G. M. Whitesides, *Adv. Mater.* **10**, 571 (1998).
18. The precursor solution has the same composition as used in the preparation of mesoporous silica films, which consisted of (in molar ratios) 0.008 to 0.018 poly(ethylene oxide)-*b*-poly(propylene oxide)-*b*-poly(ethylene oxide) ($EO_{20}PO_{70}EO_{20}$, designated P123), 1 tetraethoxysilane (TEOS), 20 to 60 ethanol (EtOH), 0.01 to 0.04 HCl, and 5 to 10 H_2O, 0 to 0.001 Rh6G.
19. The hexagonal order, which cannot be assigned by the x-ray patterns alone, was also evidenced by transmission electron microscopy on calcined samples.
20. M. Trau *et al.*, *Nature* **390**, 674 (1997).
21. M. D. McGehee *et al.*, *Phys. Rev. B* **58**, 7035 (1998).
22. F. Hide *et al.*, *Science* **273**, 1833 (1996).
23. S.-X. Qian, J. B. Snow, H.-M. Tzeng, R. K. Chang, *Science* **231**, 486 (1986).
24. U. Vietze *et al.*, *Phys. Rev. Lett.* **81**, 4628 (1998).
25. J. M. McKiernan, S. Yamanaka, B. Dunn, J. I. Zink, *J. Phys. Chem.* **94**, 5252 (1990).
26. E. T. Knobbe, B. Dunn, P. D. Fuqua, F. Nishida, *Appl. Opt.* **29**, 2729 (1990).
27. H. Yanagi, T. Hishiki, T. Tobitani, A. Otombo, S. Mashiko, *Chem. Phys. Lett.* **292**, 332 (1998). Rh6G-doped SiO_2 films were also investigated in this report. However, waveguiding on a glass substrate could only be achieved in mixed TiO_2-SiO_2 systems.
28. B. Dunn and J. Zink, *Chem. Mater.* **9**, 2280 (1997).
29. F. P. Schäfer, Ed., *Topics in Applied Physics*, vol. 1, *Dye Lasers* (Springer-Verlag, New York, 1973), pp. 158–160.
30. Very recently, a high degree of separation of guest molecules in MCM-41–type materials highly doped with phthalocyanines was reported [M. Ganschow, D. Wöhrle, G. Schulz-Ekloff, *J. Porphyrins Phthalocyanines* **3**, 299 (1999)].

31. Supported by the NSF under grants DMR 95-20971 (G.D.S.) and CTS-9871970 (B.F.C.) and by the U.S. Army Research Office under grants DAAH04-96-1-0443 (G.D.S. and B.F.C.) and DAAH04-95-1-0102 (G.M.W.). We thank V. I. Srdanov for fruitful discussions and help during this work. G.W. is on leave from the Karl-Franzens-University Graz and supported by a Erwin-Schrödinger scholarship (Fonds zur Förderung der wissenschaftlichen Forschung, J 1643-CHE). This work made use of Materials Research Laboratory Central Facilities supported by the NSF under award DMR-9632716. We thank BASF (Mt. Olive, NJ) for providing the block copolymer surfactants.

15 July 1999; accepted 22 November 1999